Cerebral Cortex, March 2019;29: 1280–1290

doi: 10.1093/cercor/bhy033
Advance Access Publication Date: 16 February 2018
Original Article

ORIGINAL ARTICLE

Cytoskeletal Associated Filamin A and RhoA Affect Neural Progenitor Specification During Mitosis

Gewei Lian, Timothy Wong, Jie Lu, Jianjun Hu, Jingping Zhang and Volney Sheen

Department of Neurology, Beth Israel Deaconess Medical Center and Harvard Medical School, Boston, MA 02115, USA

Address correspondence to Volney Sheen, Department of Neurology, Beth Israel Deaconess Medical Center and Harvard Medical School, 330 Brookline Avenue, Boston, MA 02215, USA. Email: vsheen@bidmc.harvard.edu

Abstract

Neural progenitor proliferation and cell fate decision from self-renewal to differentiation are crucial factors in determining brain size and morphology. The cytoskeletal dependent regulation of these processes is not entirely known. The actin-binding filamin A (FlnA) was shown to regulate proliferation of progenitors by directing changes in cell cycles proteins such as Cdk1 during G2/M phase. Here we report that functional loss of FlnA not only affects the rate of proliferation by altering cell cycle length but also causes a defect in early differentiation through changes in cell fate specification. FlnA interacts with Rho GTPase RhoA, and FlnA loss impairs RhoA activation. Disruption of either of these cytoskeletal associated proteins delays neurogenesis and promotes neural progenitors to remain in proliferative states. Aurora kinase B (Aurkb) has been implicated in cytokinesis, and peaks in expression during the G2/M phase. Inhibition of FlnA or RhoA impairs Aurkb degradation and alters its localization during mitosis. Overexpression of Aurkb replicates the same delay in neurogenesis seen with loss of FlnA or RhoA. Our findings suggest that shared cytoskeletal processes can direct neural progenitor proliferation by regulating the expression and localization of proteins that are implicated in the cell cycle progression and cell fate specification.

Key words: actin, cell fate specification, cortical development, degradation

Introduction

During cortical development, neural progenitors undergo self-renewal and differentiation in a precise spatiotemporal fashion to generate the appropriate number of neurons and glia. At early stages, the neuroepithelial cells mostly divide symmetrically to generate sufficient neural progenitors of similar fate for the expansion of the neuroepithelial plane and the later production of neurons (Rakic 1988; Kriegstein and Gotz 2003; Kriegstein and Noctor 2004; Geschwind and Rakic 2013). As development progresses, the neuroepithelial cells begin to be progressively biased toward asymmetric division to generate one self-renewed progenitor and another differentiating intermediate progenitors (basal progenitors) or post-mitotic neurons (Bystron et al. 2008; Toledano and Jones 2008). The intermediate (or basal) progenitors migrate into subventricular zone (SVZ) and terminally divide to generate 2 neurons. The post-mitotic neurons attach and migrate along radial glial scaffolds out of the expanding ventricular zone (germinal zone) creating a new overlying cortical layer of cells (Gotz and Huttner 2005; Bystron et al. 2008). The laminar position of neurons is characteristic of their birthdate, such that younger neurons migrate past their older counterparts to form the more superficial layers of the cortex (Frantz and McConnell 1996). At later stages of corticogenesis, most of neural progenitors adopt symmetric division to generate terminal neurons and then the remained progenitors begin to differentiate into astrocytes (Gotz and Huttner 2005; Caviness et al. 2009). Thus, the cell fate decision of neural progenitors from self-renewal to differentiation is a crucial factor in determining the morphology and size of the brain.

Subtle changes in cell specification could cause various brain malformations during cortical development, such as microcephaly and macrocephaly (Sarkisian et al. 2002; Chenn and Walsh 2003; Tungadi et al. 2017). Moreover, it would not be unexpected for cytoskeletal dynamics to play some vital role in cell fate specification. For example, the actin effector RhoA promotes contractile ring dynamics, and is involved in mitotic spindle positioning and cleavage furrow ingression (Sarkisian et al. 2002; Bakal et al. 2005; Birkenfeld et al. 2008; Chang et al. 2008). RhoA inactivation favors mitotic spindle oriented parallel to the ventricular surface (horizontal mitotic spindle) such that dividing cells have a vertical cleavage furrow (Roszko et al. 2006). The increased proportion of vertical cleavage furrows would lead to ingression along the apical-basal axis, which should promote symmetric proliferative divisions of apical progenitors. Recent studies revealed that dysfunction of RhoA caused multiple disorders during cortical development, like exencephaly, ventricular heterotopia (VH), and double cortex, etc. (Katayama et al. 2011, 2013; Cappello et al. 2012), some of which were relevant to the role of RhoA on mitotic spindle orientiation.

Alterations in actin-dependent vesicle trafficking provide another means to direct neurogenesis. Human mutations in the actin-binding Filamin A (FLNA) cause periventricular heterotopia (PVH), a disorder of neural stem cell development that is characterized by disruption of progenitor adhesion along the ventricular epithelium and subsequent formation of ectopic neuronal nodules (Fox et al. 1998; Ferland et al. 2009). In mice, loss of function in FlnA and the actin-nucleating Formin 2 (Fmn2) leads to a reduction in brain size by disrupting endocytosis of receptors at the cell surface, including the canonical Wnt associated Lrp6 receptor(Lian et al. 2016). Receptor instability impairs β-catenin activation and nuclear incorporation leading to a reduction in neural proliferation. During the cell cycle, FlnA loss impairs degradation of cyclinB1/Cdk1 associated proteins, thereby inhibiting G2-M phase progression (Lian et al. 2012). This prolongation lengthens the cell cycle and effectively slows the proliferative rate of progenitors and contributes to the smaller brain size seen in the FlnA null mice. Collectively, actin-dependent vesicle trafficking provides the structural framework to direct the localization and expression of various proteins involved in neural proliferation.

Here we show that FlnA not only directs neural proliferation but also neural specification. FlnA loss promotes vertical cleavage planes in neural progenitors during cell division and leads to an increase in the number of daughter progeny remaining in the cell cycle (symmetric division), as well as a reduction in neural cells expressing early neuronal markers. Mechanistically, FlnA binds RhoA, and FlnA loss leads to diminished basal RhoA activation levels and limits sustained RhoA activation following extracellular matrix activation. In utero electroporation of a dominant negative RhoA similarly leads to dividing cells undergoing symmetric divisions, and giving rise to proliferating daughter progeny (remaining as progenitors as opposed to post-mitotic cells). Both FlnA loss of function and dominant negative RhoA lead to aberrant mitotic localization and degradation of Aurora kinase b (Aurkb). Aurkb is serine/threonine kinases that is essential for G2/M phase transition, coordinates with Rho kinase, and is involved in cytokinesis (Terada et al. 1998; Kawajiri et al. 2003; Kim et al. 2007; Tsuno et al. 2007). Overexpression of Aurkb results in the same shift toward increased proliferating progenitors. The current studies suggest that FlnA directly regulates RhoA activation to affect downstream localization and expression of cell fate and cytokinesis determinants such as Aurkb and that disruption of these actin associated processes can effect cell fate specification and differentiation. Prior work has shown that FlnA regulates the temporal progression through the cell cycle (Lian et al. 2012). Collectively, these findings demonstrate a shared cytoskeletal dependent mechanism that influences neural progenitor proliferation and differentiation through regulation of both cell cycle progression and cytokinesis.

Materials and Methods

Mice

The *Dilp2* mouse strain was obtained from the Comparative and Developmental Genetics Dept. MRC Human Genetics Unit, Edinburgh EH4 2XU, UK. FlnA-loxp mice were obtained from Dr Christopher A. Walsh laboratory at Children's Hospital, Harvard Medical School.

The *Dilp2* mice harbor a T to A point mutation in the *FlnA* gene, leading to a stop codon in exon 46 (Fig. S1*A*). The nonsense mutation mediated *FlnA* mRNA degradation (Fig. S1*B*), causing undetectable FlnA protein levels using either N- (domain 4) or C-terminal (last domain) FlnA antibodies (Fig. S1*C*,*D*). H&E staining showed that the brain size in E15 *Dilp2* ($FlnA^{y/-}$) embryo was smaller than that in WT ($FlnA^{y/+}$) embryo (Fig. S1*E* upper panel). More prominently, the cortical plate and intermediate zone, where postmotitic neurons reside, were much thinner in the FlnA-null mutant cortex, suggesting some impairment in neurogenesis due to FlnA functional loss.

All mouse studies were performed under approval from the Institutional Animal Care and Use Committees of Harvard Medical School, Beth Israel Deaconess Medical Center, and Albany Medical College in accordance with The National Institutes of Health Guide for the Care and Use of Laboratory Animals.

Constructs and Antibodies

The pCMV5 expression vectors carrying Flag-tagged WT and constitutively active RhoA, Cdc42 and Rac1 were gifted from Dr Takaya Satoh at Kobe University graduate School of Medicine. The constructs for GST-tagged WT and constitutively-active RhoA, Cdc42 and Rac1 were obtained by cutting these pCMV5 expression vectors and inserting the genes into pGEX-6p-3 vector with GST tag. Myc-tagged FLNA c-terminal-expression construct was obtained by inserting Myc-tagged FLNA c-terminal PCR fragment (aa2167–aa2647, protein code: P21333 on NCBI website) into pCDNA3.1 vector. HA-tagged Cre and GFP constructs for electroporation were purchased from Addgene Company. The following antibodies with corresponding dilutions were used for the studies: mouse anti-BrdU (1:100, Calbiochem) and rat anti-BrdU (1:150, Serotec, cat. MCA2060), rabbit anti-Ki-67 monoclonal antibody (1:200, Epitomics, cat. 4203-1), rabbit anti-PH3 polyclonal antibody (1:250, Millipore cat: 06–570), rabbit anti-Sox2 (1:250, Epitomics, cat. 2683-1), rabbit anti-Tbr-1 and anti-Tbr-2 (1:150, Abcam, cat. ab31940, ab23345), mouse anti-E-cadherin and anti-N-cadherin (1:100, BD Biosciences, cat. 610181 and 610920), α-tubulin (Santa Cruz, cat. 32293), rat anti-β1 integrin (1:100, Millipore, cat: MAB 1997), FLNA (1:200, Epitomics cat. 2242-1), mouse ant-RhoA(1:50, Santa Cruz, clone:26C4, cat: sc-418) and rat anti-RhoA (clone: lulu51) was gifted from Dr Shigenobu Yonemura at RIKEN Center for Developmental Biology, mouse anti-Tuj1 (1:200, Covance cat: MMS-435P), mouse anti-aurora b (AIM-1, 1:100, BD Bioscience, cat. 611082), cdk1(1:1000, Calbiochem,

pc25), Alexa fluor 488 or rhodamine-labeled phalloidin (1:50, Invitrogen cat. A12379 and R415). The secondary antibodies were used: dye 488 and dye 594 donkey anti-mouse antibodies (1:200), and dye 488 and dye 594 donkey anti-rabbit antibodies (1:200) from Jackson Immunoresearch.

In Vivo BrdU Labeling and In Utero Electroporation

BrdU labeling in vivo and all the embryo operations were same as those published previously (Zhang et al. 2012, 2013). Cre, RhoA or GFP plasmids were in utero electroporated into brain ventricles of E13.5 and E14 embryos as described previously (Zhang et al. 2012, 2013).

Cell Culture, Transfection, Pull-down, Immunoprecipitation and Immuno- fluorescence

Neuro-2 and CHP-100 cells were cultured in 10% FBS/DMEM medium; WT, null FlnA and FlnA-loxp neural progenitor cells were cultured in neural progenitor culture medium (Invitrogen). Plasmid transfection, pull-down, immunoprecipitation and immuno-fluorescence were performed as described previously (Zhang et al. 2012, 2013). Briefly, for pull-down assays, myc-tagged FLNA C-terminal was expressed in Neuro-2 cells for 24 h, and pulled-down with purified GST or GST-fused Rho GTPase beads. Pulled-down myc-FLNA was detected by Western blot with anti-myc antibody (Invitrogen Cat: 13–2500). For co-immunoprecipitation assays, myc-tagged FLNA C-terminal or full-length FLNA construct was co-transfected with Flag-tagged Rho GTPase (constitutively-active and WT-RhoA, Rac1 and Cdc42) constructs into Neuro-2 cells for 24 h. Full-length FLNA and FLNA C-terminal were co-immunoprecipitated with anti-Flag antibody (Sigma Cat: F3165), and detect by Western blot with anti-FLNA antibody (Abcam Cat: ab76289). For RhoA activation assays, WT and null FlnA neural progenitors were plated to 10 ug/ml laminin-coated dishes and incubated at 37 °C for different time. Cells were dissolved into lysis buffer and active RhoA was pulled-down using GST-Rhotekin-RBD beads (Cytoskeleton, Inc).

For Western blot experiments, protein samples were loaded onto 8–12% SDS-PAGE gels for electrophoresis, and transferred onto PVDF membrane (Bio-rad, cat.162–0177). Membranes were incubated with primary antibodies overnight at 4 °C, and with HRP-conjugated secondary antibodies (1:3000, Jackson Immunoresearch) for 2 h. Signals were detected using LumiGOLD ECL detection kit (Signagen Laboratories, cat. SL100309).

Northern Blot

The substrates for RNA probe synthesis were synthesized by polymerase chain reaction (PCR) using total cDNA from mouse brain, FlnA primers, forward: AGAACACA-TTCACCCGCTGG and reverse: AGGACATAGGCCTGGGGCAC, and GAPDH primers, forward: AGGCCGGTGCTGAGTATGTC and reverse: TGCCTGCTTCACCACC TTCT. Biotin-labeled RNA probes for FlnA and GAPDH were synthesized by NEB T7 RNA polymerase. Northern blot assays were performed using Northern blot kit from KPL, Inc and the procedure followed the kit manual.

Quantitative Analysis

The quantitative analysis was performed as described previously (Zhang et al. 2012, 2013). Briefly, to quantify the number of positively labeled cells on serial tissue sections, cell number was quantified using Image J software (NIH). Cleavage furrow orientation, which refers to the angle between cleavage furrow plane and apical surface of cortical ventricle, was measured by drawing the lines along the cleavage plane and apical lining. Three coronal sections of one FlnA-null brain were compared with 3 homotopic sections of one FlnA-WT brain in a same litter. A total of more than 4 sets of experimental and control E14–E15 embryonic brains were used for analyses (i.e., $n \geq 4$ for FlnA-WT brains and FlnA-null brains). Data are represented as the mean ($n \geq 4$) ± STDEV for BrdU, Ki-67, Tbr-1, Tbr-2 and Sox2. *P*-value was calculated by Excel software. Significance was determined using a paired Student's *T*-test.

Results

Alteration of Neural Progenitor Fate Decision Due to FlnA loss Contributes to the Neurogenesis Defect

We had previously shown that loss of FlnA leads to a prolongation in cell cycle during G2/M phase, such that a neurogenesis defect might result in delayed formation of the cortical plate (Lian et al. 2012). To further verify these observations, we quantified the number of neural cells expressing several layer-specific markers in E15 cortex. The staining of the neural progenitor marker Sox2 showed that the neural progenitor population was not significantly different between WT and FlnA$^{y/-}$ cortices at E15 (Fig. S2A–C). Staining for the intermediate progenitor marker Tbr-2 displayed a trend toward decreased numbers of differentiating progenitors in FlnA$^{y/-}$ cortex. However, significantly fewer Tbr-2^{+} cells were seen in the intermediate zone of FlnA$^{y/-}$ brain (arrow in Figs. S2A,B). Lastly, staining for Tbr-1, a neuronal marker of early born neurons showed that the number of Tbr-1^{+} neurons in deeper layers of the cortical plate was significantly decreased (14% less) in FlnA$^{y/-}$ cortex. Furthermore, the later-born neuronal layer above the Tbr-1^{+} neuronal layer was evident in WT cortex but not in null FlnA cortex. Collectively, our prior studies and the above data supported the hypothesis that FlnA loss could cause a defect in neurogenesis within the cerebral cortex at the mid-gestation.

A neurogenesis defect might also result from altered cell fate decision with daughter cells adopting precursor identities rather than assuming either intermediate progenitor of post-mitotic neuronal fates. A reduction in proliferation due to cell cycle changes should proportionally reduce the sizes of both the neuronal (cortical plate) and neural progenitor pools (ventricular zone) under a prerequisite of identical fate decision, while the alteration of cell fate decision would change the thickness ratio of the cortical plate to ventricular zone regardless of proliferation. We therefore analyzed the sizes of the neuronal and neural progenitor's pools. A static observation by Tuj1 (neuronal marker) and Sox2 (neural progenitor marker) co-staining of cerebral cortices at different developmental stages (E14, E15 and E18) indicated that the neuronal proportion in FlnA$^{y/-}$ cortex was significantly less than that in WT cortex (Fig. 1A,B). More importantly, a temporal observation of the staining from E14 to E18 indicated that the rate of differentiation of neural progenitors was slower in FlnA$^{y/-}$ cortex compared with that in WT cortex (Fig. 1A–C), suggesting fewer neural progenitors in FlnA$^{y/-}$ cortex underwent the differentiation destiny. The trend for these different rates (Fig. 1C plot) of neuronal differentiation between null FlnA and WT neural progenitors suggested that the observed reduction in the null FlnA cortical plate thickness was not simply attributable to a reduction in proliferation due to cell cycle prolongation. The rate of decline of the relative progenitor pool in FlnA$^{y/-}$ brain was not

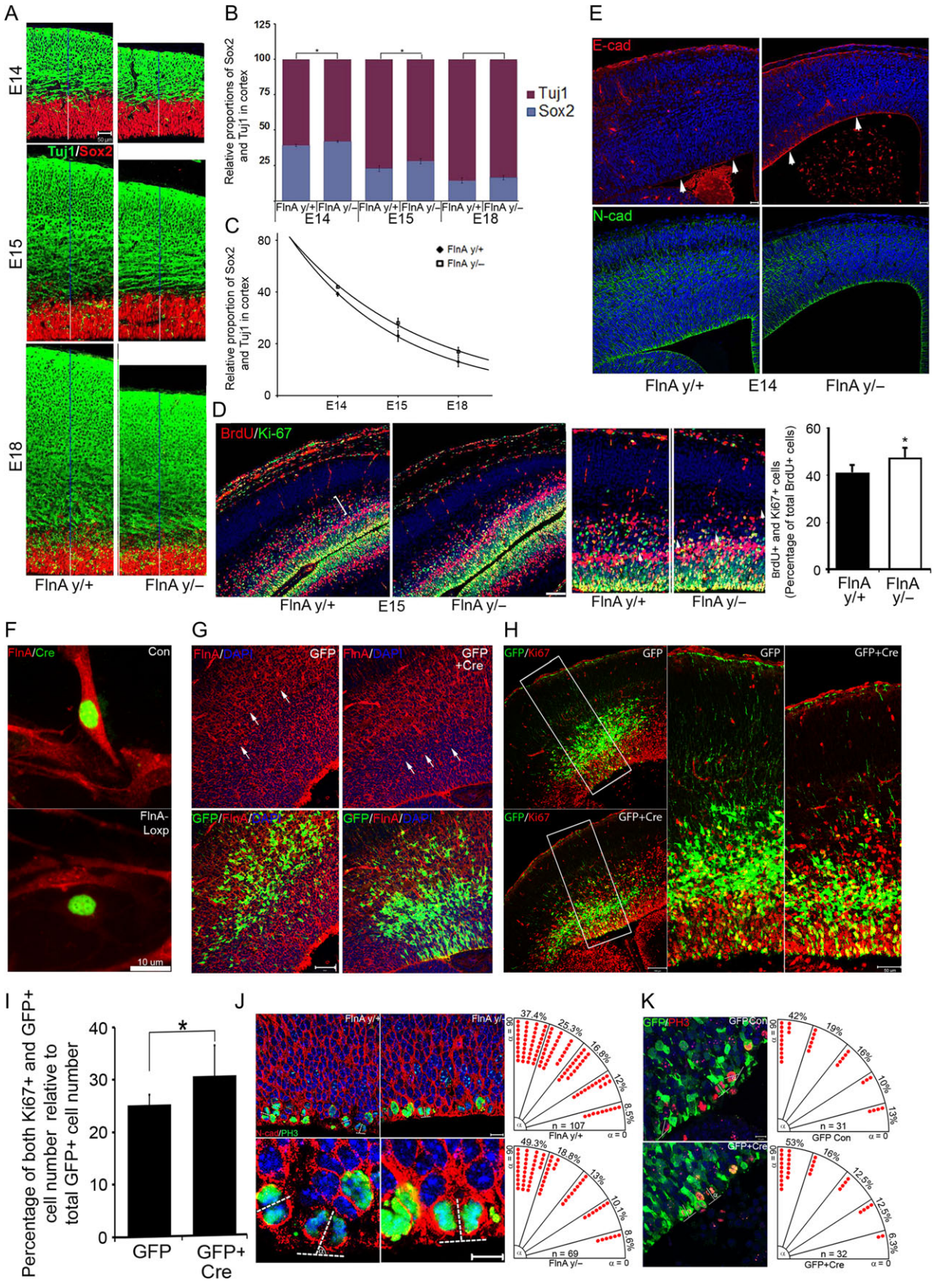

Figure 1. FlnA loss impairs neural progenitor proliferation and differentiation. (*A*) Fluorescent photomicrographs of FlnA$^{y/-}$ cortices as compared with FlnA$^{y/+}$ (WT) cortices in various-aged embryos (E14, E15 and E18). Co-immunostaining with Tuj1, a neuronal marker (fluoroscein), and Sox2, a progenitor marker (rhodamine) reveals both a reduction in the width of the cortex and an increased proportion of Sox2 to Tuj1 cells in the FlnA$^{y/-}$ mice. Scale bar = 50 μm. (*B*,*C*) The relative width

significantly different from that in WT brain during this period (Fig. 1A,B). Additionally, the changes in neuronal thickness could not be explained by cell death, as no increase in apoptosis was seen (Lian et al. 2012).

To further verify the difference in differentiation rates between FlnA$^{y/-}$ and WT neural progenitors, we pulse BrdU-labeled the embryos at E14 and analyzed the BrdU incorporation 24 h later (Figs. 1D). Co-staining of BrdU with Ki-67 (proliferating marker) showed that the proportion of BrdU$^+$, Ki-67$^+$ cells in FlnA$^{y/-}$ cortex was significantly more than that in WT cortex. Progenitors that remained in cell cycle would have been labeled with BrdU and become Ki67 positive. Conversely, the number of BrdU$^+$, Ki-67$^-$ cells above the FlnA$^{y/-}$ ventricle zone (see bracketed region) was significantly reduced compared with WT cortex. Finally, E-cadherin expression in the normal neuroepithelium progressively decreases as neural progenitor differentiation increases during corticogenesis. Staining for E- and N-cadherins showed that E-cadherin expression in the E14 null FlnA neuroepithelium was fairly robust while its expression was virtually absent in WT littermate neuroeipthelium (see white arrow heads, Fig. 1E). As a control, N-cadherin expression was unchanged (Bottom 2 panels, Fig. 1E), again implying a neuroepithelial fate change due to FlnA loss. Collectively, these initial characterization studies suggested that FlnA loss might cause an alteration in neural progenitor fate decision and a reduction in neurogenesis prior to mid-corticogenesis, although these observations would require further exploration.

Acute FlnA Loss Changes Divisional Plane Orientation of Mitotic Neural Progenitors and Impairs Neurogenesis

To further confirm the effect of FlnA on neural progenitor fate decision, we acutely inhibited FlnA expression in E13.5 FlnA-loxp embryo brains by in utero electroporation of Cre-construct. Cre expression in FlnA-loxp neural progenitors efficiently abolished FlnA expression in vitro (Fig. 1F). Additionally, FlnA expression in GFP+ Cre-expressing cells was reduced in vivo (Fig. 1G, right panel) compared with that in control GFP-expressing regions (Fig. 1G, left panel). Lastly, co-staining with anti-GFP and anti-Ki67 antibodies showed that the proportion of GFP$^+$, Ki67$^+$ cells in total GFP$^+$ cells of Cre-electroporated cortices is higher than that of control GFP-electroporated cortices (Fig. 1H,I), further supporting the conclusion that FlnA loss causes a reduction in neurogenesis through altering neural progenitor fate decision.

During early neurogenesis, the fate decision of neural progenitors is regulated by divisional plane orientation, which affects the symmetry/asymmetry of mitotic divisions and controls the distribution of cell fate determinants in 2 separating progenies, thereby dictating a cell destiny (Chia et al. 2001; Siller and Doe 2009). Based on the phenotype observed above, we asked whether FlnA functional loss could affect the divisional plane orientation in mitotic neural progenitors of E14 embryos. Co-staining of PH3 (mitotic phase marker) with N-cadherin (plasma membrane-associated adhesion marker) indicated that a greater proportion (50% above 72°) of FlnA$^{y/-}$ mitotic progenitors adopted a vertical orientation for the divisional plane verses that seen in WT cells (38%, Fig. 1J), suggesting that more FlnA$^{y/-}$ neural progenitors divide symmetrically compared with littermate WT cells. To exclude the possibility that a developmental delay due to the FlnA loss-impaired proliferation might cause the increase in symmetric division, we transiently inhibited FlnA expression in brains of loxp-FlnA E13.5 embryos by in utero electroporation of a Cre enzyme construct to observe the variation of divisional plane orientation (Fig. 1K). Similar to that seen in FlnA$^{y/-}$ embryos, transient FlnA loss caused a greater proportion of mitotic neural progenitors to adopt a destiny of symmetric division (52% in loxp-FlnA brains vs. 43% in WT brains). Thus, the alteration in divisional plane orientation due to FlnA loss was not derived from the developmental delay alone, but from other molecular mechanisms.

FlnA Specifically Binds to RhoA, and FlnA Loss Causes a Dysregulation of Integrin-Mediated RhoA Activation

FlnA binds β integrins and integrin-mediated adhesion can direct actin cytoskeletal dynamics and mitotic spindle orientation

proportions of Sox2 and Tuj1 in the cortices are quantified graphically and the best curve fit by linear regresson indicates a slower rate of differentiation for FlnA$^{y/-}$ neural progenitors, suggesting loss of FlnA also alters neural progenitor specification/differentiation. (D) Fluorescent photomicrographs of the cerebral cortices from FlnA$^{y/-}$ and WT at E15 show co-staining for BrdU (rhodamine) and Ki-67 (fluorescein). Higher magnification images and statistical analyses are seen to the right. The BrdU$^+$, Ki-67$^+$ cells and total BrdU$^+$ cells from same position-matched area of cortices were quantified. The statistical analysis (n = 4) showed that the ratio of the BrdU$^+$,Ki-67$^+$ cells in total BrdU$^+$ cells increased approximately 5% in the *FlnA* $^{y/-}$ cortex. Additionally, the number of BrdU$^+$ neurons above the *FlnA* $^{y/-}$ ventricular zone (bracketed area) is increased in WT mice, consistent with increased differentiation. Sections were counterstained with nuclear Hoechst or DAPI. Scale bar = 50 μm. (E) Fluorescent photomicrographs show that E-cadherin staining at the apical lining (arrows) of WT cortex is weaker and less prominent than the same littermate FlnA$^{y/-}$ cortex. In contrast, N-cadherin staining at the apical lining was not distinctly different. E-cadherin expression diminishes with cortical maturation, suggesting delayed differentiation in E14 FlnA$^{y/-}$ cortex. Scale bar = 50 μm. (F) FlnA expression in FlnA-loxp neural progenitor cells can be efficiently inhibited by Cre enzyme. HA-tagged Cre-construct was transfected into WT and FlnA-loxp neural progenitors and knockdown of FlnA protein at 48 hours post-transfection was confirmed by co-immunostaining with anti-FlnA (rhodamine) and anti-HA (fluoroscein) antibodies (upper panel). Scale bar = 10 μm. (G) Fluorescent photomicrographs of E13.5 cerebral cortices from control or Cre-construct electroporated embryos show a reduction (see arrows) in FlnA expression (rhodamine) in regions of Cre-expressing cells (GFP, green) compared with that in control cells containing GFP (green) only. Nuclei were counterstained with DAPI. Scale bar = 50 μm. (H) Transient loss of FlnA through Cre cleavage in FlnA-loxp brains causes a reduction in neural progenitor differentiation at E13.5. Fluorescent photomicrographs of the cerebral cortices show increased numbers of GFP$^+$ and Ki67$^+$ cells (yellow) in Cre-expressing brains, suggesting that transient FlnA loss inhibits neural progenitor differentiation. Higher magnification images are seen to the right. Scale bars = 100 and 50 μm. (I) Statistical analyses on experiments from panel H are shown graphically confirming an increase in the number of cells remaining as progenitors following impairment of FlnA function. (J) Fluorescent photomicrograph of the ventricular zones from the cerebral cortices of E14 FlnA null and WT mice. FlnA functional loss leads to an increase in the number of mitotic neural progenitors with a vertical cleavage plane orientation, relative to the apical lining. Co-immunostaining with N-cadherin and phospho-histone 3(PH3) allows for orientation of dividing neural progenitors in ventricular zone of E14 brains. The lower panel is a higher magnification of upper panel. Scale bar = 10 μm. The angle (α) for the cleavage plane relative to the apical lining was quantified for each dividing neural progenitor. The numerical angle numbers (n = 107 for FlnA$^{y/+}$ and N = 69 for FlnA$^{y/-}$) were subgrouped into 5 equal divisions in the right fan. Statistical analysis revealed that the number of dividing neural progenitors with vertical cleavage plane (>72°) in E14 FlnA$^{y/-}$ cortical ventricles is significantly increased compared with that in littermate WT cortical ventricles ($P < 0.05$). (K) Transient FlnA loss similarly promoted a vertical cleavage plane orientation in dividing neural progenitors. HA-Cre and GFP constructs were in utero co-electroporated into E13.5 WT and FlnA-loxp brain ventricles and stained for the mitotic marker PH3 (rhodamine) to capture dividing neural progenitors. The angles for the cleavage planes in GFP-expressing neural progenitors were measured (n = 31 for GFP control and n = 32 for Cre-construct) and subgrouped into 5 equal divisions in the right fan. Statistical analysis shows a greater number of Cre and GFP co-transfected neural progenitors adopting a vertically-oriented cleavage plane (>72°), suggesting that acute loss of FlnA can disrupt symmetric versus asymmetric division ($P < 0.05$).

(Lechler and Fuchs 2005; Kiema et al. 2006; Marthiens and ffrench-Constant 2009; Streuli 2009). Therefore, a reasonable hypothesis for our phenotypic observation is that FlnA might regulate divisional plane orientation in mitotic neural progenitor cells and influence cytokinesis through an integrin-mediated pathway. Because integrin regulates actin re-orgaization through Rho GTPases, such as RhoA, Rac1 and Cdc42 (Huveneers and Danen 2009), we first examined if the Rho GTPases could interact with FlnA in Neuro2A cells. Both WT and constitutively-active RhoA, but not Rac1 or Cdc42, could pull-down FlnA C-terminal (Fig. 2A, left panel). Co-immunoprecipitation assays displayed a similar result (Fig. 2A, middle panel). Lastly, full-length FlnA displayed an enhanced interaction with RhoA but not Rac1 and Cdc42 by co-immunoprecipitation (Fig. 2A right panel). We further found that RhoA co-localized with FlnA in E13.5 brain cortex, especially along the apical lining (Fig. 2B). Co-staining of RhoA with FlnA on cultured CHP-100 cells (neuroblastoma cells) showed that RhoA was co-localized with FlnA at focal adhesions (Bottom panels, Fig. 2B). Thus, FlnA specifically bound to and overlapped with RhoA at cell adhesion sites along the apical lining.

Several observations suggest that FlnA can regulate RhoA activation and localization. Treatment of FlnA containing cells with fetal calf serum (FCS) has been shown to induce FlnA

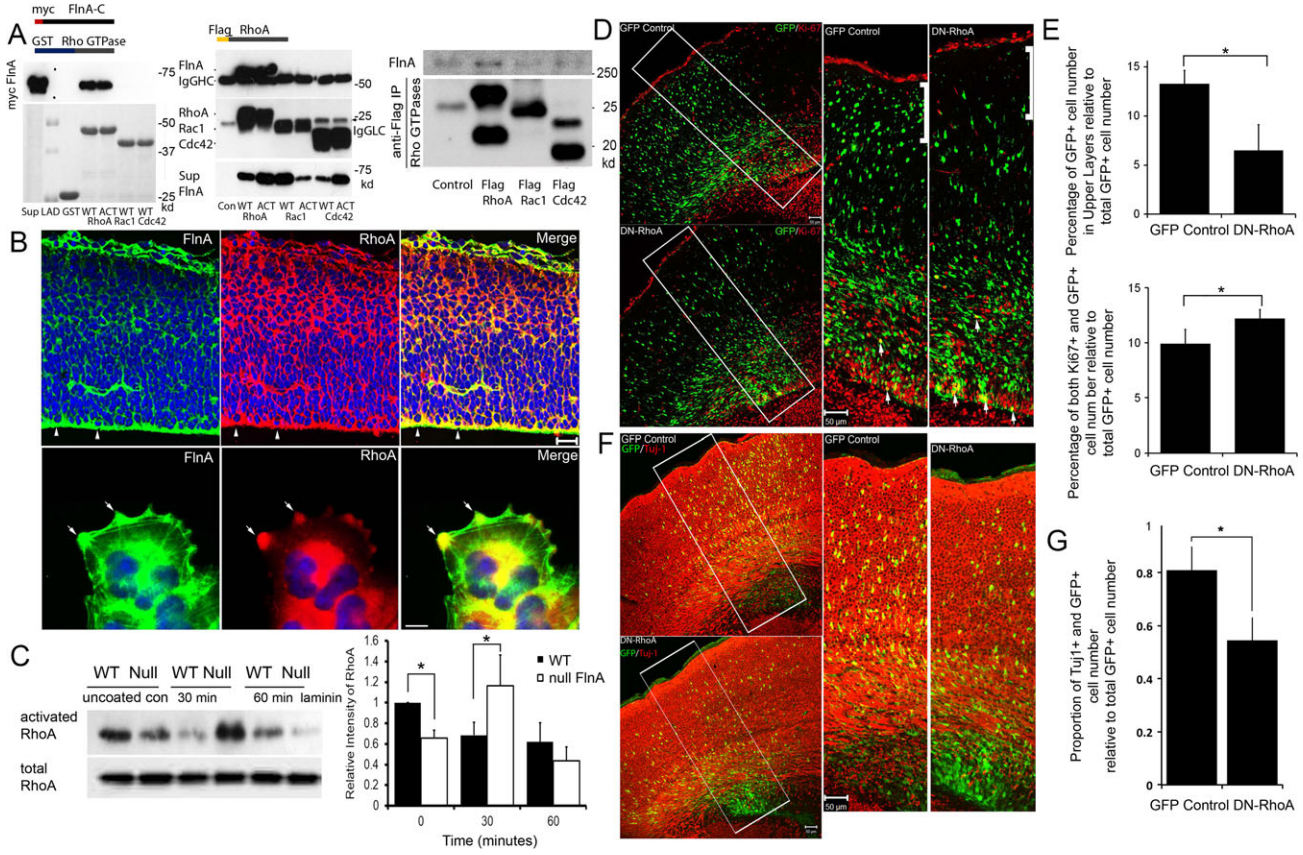

Figure 2. FlnA physically interacts with RhoA and regulates RhoA activation to direct neural progenitor proliferation and differentiation. (*A*) Rho GTPase pull-down assays shows that only active (ACT) or WT-RhoA but not Cdc42 or Rac1 pulls down FlnA by Western blot (left panel) in Neuro2A cells. Conversely, RhoA is co-immunoprecipitated by FlnA C-terminal whereas WT or active Cdc42 and Rac1 did not show any significant binding interaction on Western blot (middle panel). Lastly, full-length FLNA can be co-immunoprecipitated by Flag-RhoA, whereas Flag-Rac1 and Cdc42 cannot (right panel). SUP = supernatant, LAD = molecular weight ladder. Control reflects empty FLAG vector lacking the Rho GTPase constructs followed by pull-down with anti-FLAG antibody and probing for FlnA. (*B*) Fluorescent photomicrographs of cerebral cortex demonstrate FlnA overlapping expression with RhoA in E14 brain cortex, especially, along the apical lining by co-immunostaining and at focal adhesion sites (arrows) of neuroblastoma cells. (*C*) FlnA loss impairs RhoA activation. At baseline, activated RhoA levels are diminished in null FlnA mice. Following laminin activation, RhoA GTPase dramatically increases in the FlnA$^{y/-}$ neural progenitors by 30 min but also declines more precipitously than WT progenitors at 60 min. WT and FlnA$^{y/-}$ neural progenitors are plated on uncoated (uncoated con) or laminin-coated dishes and RhoA activation is assessed at varied time points (30 and 60 min post plating). Upper band corresponds to activated RhoA, and lower band reflects total RhoA (T-RhoA) for loading control. The graph at the right represents mean ± SD values from 5 independent Western blot assays. (*D*) Fluorescent photomicrographs of E14 cerebral cortices 24 h after in utero electroporation of control GFP or dominant negative RhoA (DN-RhoA). Fewer neural cells expressing the DN-RhoA construct reach the cortical plate from the ventricular zone within this time frame, suggesting either impaired migration or diminished neurogenesis. The electroporations specifically target mitotic, proliferating progenitors at the ventricular lining. Progenitors which are therefore GFP$^+$ but Ki67- have exited the cell cycle. Higher magnification images and statistical analyses are seen to the right. Co-immunostaining was performed with anti-Ki-67 (marker of cells that remain in the cell cycle) and GFP (marker that initially captures proliferating progenitors) antibodies. The number of GFP$^+$ cells that are situated above the ventricular zone is increased in the electroporated GFP control mice (brackets in higher magnification), consistent with increased differentiation. (*E*) The GFP$^+$,Ki-67$^+$ cells and total GFP$^+$ cells from same position-matched area of cortices were quantified. The statistical analysis ($n > 4$) show that the ratio of the GFP$^+$, Ki-67$^+$ cells in total GFP$^+$ cells is increased approximately 25% in the DN-RhoA electroporation construct versus control. These observations mirror the FlnA loss of function cortical phenotypes and reinforce the likely functional interaction between FlnA and RhoA. Scale bar = 50 μm. (*F*) Fluorescent photomicrographs of GFP (fluorescein) expressing neural cells following electroporation of control GFP or DN-RhoA into lateral ventricles of E13.5 cerebral cortex and staining for early neuronal markers (Tuj1). Acute RhoA inhibition leads to reduction of early born neurons within 72 h, similar to that seen with loss of FlnA. (*G*) Quantification of neurogenic fates is graphically summarized. * = $P < 0.05$.

phosphorylation and delivery of proteins to the cell membrane (Zhang et al. 2012). With FCS treatment in FlnA-replete A7 cells, RhoA redistributes toward the membrane periphery and cells adopt a retracted, more rounded morphology (Fig. S3A). We further found that integrin β1 was highly expressed in developing brain cortex (E14), especially along the ventricular zone, and mainly at the apical membrane of mitotic neural progenitors (Fig. S3B). Given the similar localization for β1 integrin, FlnA and RhoA along the ventricular zone and within cell focal adhesion sites, we examined if laminin-1 (an integrin ligand in the brain) could mediate RhoA activity in neural progenitor cells in a FlnA-dependent way. RhoA activity was higher in unstimulated WT cells (Fig. 2C lanes 1 and 2). However, its activity in WT cells decreased 30 min later when the cells were plated on laminin-1 coated dishes. In contrast, FlnA null cells exhibited increased RhoA activity under the same condition (Fig. 2C lanes 3 and 4). Sixty minutes post stimulation, RhoA activity in both WT and FlnA-null cells recovered to baseline levels, where WT cells maintained higher basal RhoA activity. Coincident with this pattern of RhoA activation, lammellipodia and stress fiber formed well in WT cells, but these actin structures were poorly organized in FlnA null cells (Fig. S3C, arrows point to lammellipodia and arrow heads to stress fibers). Further, WT cells rapidly spread on ECM-coated dish whereas FlnA null cells appeared to poorly spread (data not shown). No changes in RhoA activation levels were seen following plating on uncoated dishes (Fig. S4). Thus, FlnA loss led to a dysregulation of RhoA activation and an alteration of cell function.

Loss of RhoA Activity Impairs Neural Progenitor Cell Differentiation

RhoA is a member of the Ras superfamily of proteins that regulate cytoskeletal rearrangements in mammalian stem cells. It has been reported that they facilitate many critical cellular functions, including self-renewal, adhesion and migration. Therefore, it is reasonable to expect their involvement in regulating neural progenitor proliferation, and subsequent cortical development. As FlnA and RhoA interact physically and are functionally dependent, we asked if the loss of RhoA activity could also impair neural progenitor differentiation in the same manner as seen with loss of FlnA function. We performed in utero electroporation of E14 brains with GFP control and DN-RhoA, and quantified layer-specific markers 24 h later (Fig. 2D). Significantly fewer GFP+ cells were present in the cortical plate of DN-RhoA, compared with control GFP (white brackets, Fig. 2D). To ascertain whether the observation was a result of reduced differentiation, we quantified the number of cells that were GFP^+ and $Ki67^+$ (proliferation marker). Positive staining for both markers indicates that cells are proliferating and have not undergone differentiation into neurons. Our results showed that DN-RhoA expression results in more $Ki67^+$ and GFP^+ cells than its control (Fig. 2E). Under the presumption that more cells remained in cell cycle and did not undergo differentiation into post-mitotic neurons, we would expect a significant decline in the neuronal population in the cortical plate. Cells that have differentiated into post-mitotic neurons would be GFP^+ and $Tuj1^+$ (early neuronal marker). Our results showed a smaller proportion (26% less) of GFP^+ and $Tuj1^+$ cells in the DN-RhoA cortex, compared with GFP control (Fig. 2F,G). Collectively, these results suggest that loss of RhoA activity causes neural progenitor cells to remain in cell cycle, as well as reduce their maturation into post-mitotic neurons.

FlnA Regulates Aurora kinase B (Aurkb) Localization and Expression During Cell Division

FlnA promotes M phase progression through regulating Cdk1 activity and the activation of Cdk1 and Aurora kinases are indispensable for asymmetric division of neuroepithelial cells ((Palacios et al. 2001; Tio et al. 2001; Lian et al. 2012)). Aurkb levels peak during G2/M phase and the kinase is critical for cytokinesis. Thus, we examined the localization of Aurkb in dividing neural progenitors (Fig. 3A). In metaphase, Aurkb was exclusively localized to the chromosomal DNA in both WT and FlnA null cells. In anaphase and telophase, it translocated to the cleavage plane in WT cells but still was present on chromosomes in FlnA null cells (Fig. 3A, white arrow), indicating a delay or disruption in its translocation. Also, a significantly greater proportion of Aurkb was associated with chromosomes in FlnA null cells than control cells during anaphase and telophase (Fig. 3A, graph). With the observation that FlnA affects Aurkb distribution and mediates G2/M phase progression of neural progenitors, we sought to determine if FlnA also regulates the expression levels of Aurkb in G2/M phase. Nocodazole was used to synchronize neural progenitors to G2/M phase and its release allows progenitors to undergo G2/M phase progression into G1 phase. Western blot analyses showed that the Aurkb expression levels in FlnA-null cells declined more slowly relative to that seen in WT cells (Fig. 3B) as cell progressed through the cell cycle. Overall, these observations suggest that FlnA plays some role in regulating the segregation of cell fate-determining proteins such as Aurkb and enhances its expression during mitosis.

Impaired clearance of Aurkb could be due to enhanced protein synthesis or delay in its degradation. We therefore asked whether use of a protein synthesis inhibitor cyclohexamide would alter the expression levels of Aurkb. Pretreatment with cyclohexamide resulted in persistently elevated levels of Aurkb in null FlnA neural progenitors, relative to WT control at similar time points (Fig. 3C). The current results support the notion that FlnA influences the spatiotemporal distribution and processing of various proteins involved in cell specification and cytokinesis such as Aurkb in affecting neuroprogenitor differentiation by impairing degradation.

The loss of RhoA activity impairs translocation and degradation of Aurora B during mitosis

Given the FlnA-RhoA interaction, we asked if RhoA plays a similar role in the translocation and processing of Aurkb during cell cycle. We transiently transfected neural progenitors, and observed the distribution of Aurkb following nocodazole release in prometaphase, metaphase and anaphase (Fig. 4A). We found that DN-RhoA cells demonstrated a diffuse cytoplasmic distribution of Aurkb in prometaphase, metaphase and anaphase (Fig. 4A, white arrow heads). Conversely, control cells demonstrated tight association of Aurkb and chromosomes during prometaphase and metaphase (Fig. 4A, white arrows). Later, Aurkb translocated to the cleavage plane during anaphase (Fig. 4A, white arrows). To quantify the effect of DN-RhoA on Aurkb translocation, we measured the proportion of Aurkb in the cleavage furrow relative to total Aurkb during anaphase. Our results indicated that significantly less (approximately 37%) Aurkb was localized to the cleavage plane in DN-RhoA cells, compared with control. Western blot analysis also showed that the level of Aurkb is higher in DN-RhoA, compared with its WT counterpart (Fig. 4B). A similar increase is seen Cdk1, suggesting that like FlnA, RhoA can

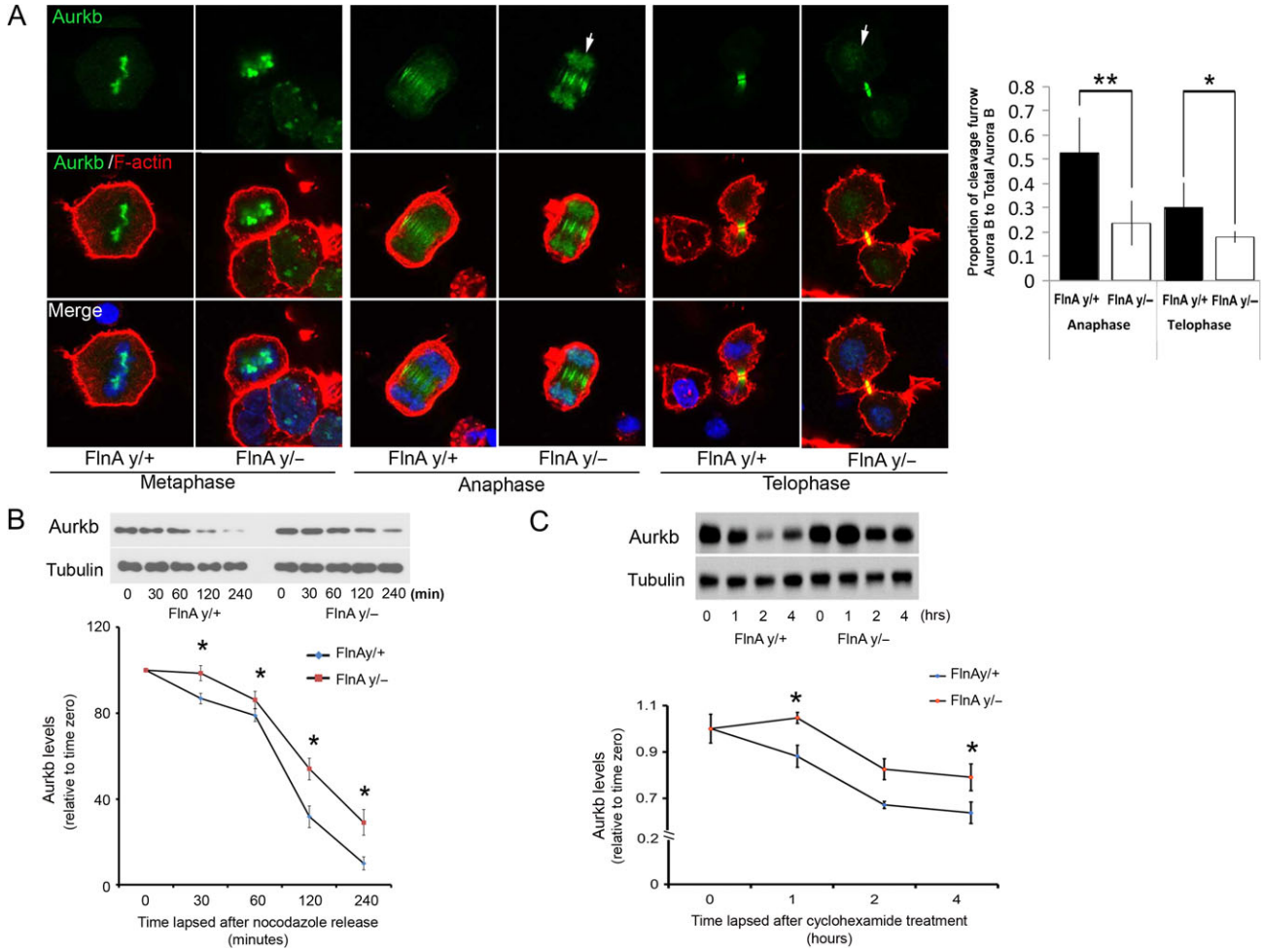

Figure 3. FlnA loss of function disrupts translocation and degradation of Aurora B (Aurkb) kinase in mitotic neural progenitors. (*A*) Fluorescent photomicrographs show immunostaining for Aurkb and F-actin within dividing neural progenitors during various stages of the cell cycle. Aurkb translocation in FlnA$^{y/-}$ neural progenitors (see the arrows in anaphase and telophase cells) is impaired compared with that in WT cells. Changes in Aurkb localization are quantified graphically to the right during anaphase and telophase. Our results indicate that the translocation of Aurkb to the cleavage furrow in FlnA-null neural progenitors is impaired, compared with WT. * = $P < 0.05$, ** = $P < 0.01$. (*B*) Western blot analyses show the delay in the decrease of Aurkb levels in FlnA$^{y/-}$ neural progenitors at various times after nocodazole release compared with WT control. Changes in Aurkb expression levels are quantified graphically below ($n > 3$ blots, $P < 0.05$% for all time points). (*C*) FlnA-dependent decline in Aurkb levels is due to degradation and not protein synthesis. WT and null FlnA neural progenitor cells were treated with 100 ug/ml cycloheximide (CHX, a protein synthesis inhibitor) for various time lengths (0, 1, 2, and 4 h). The representative blot indicated that Aurkb degradation in WT cells was faster than that in null FlnA cells. Data are summarized graphically below from 3 independent Western blot assays. * = $P < 0.05$.

also influence cell cycle proteins and proliferation. Collectively, our results suggest that DN-RhoA impairs both localization of Aurkb to the cleavage furrow and its degradation. The observed phenotype is consistent with that of FlnA null cells, again suggesting that these cytoskeletal proteins can influence proteins implicated in cell cytokinesis and neural differentiation.

Aurora B Overexpression Causes Neural Progenitor Cells to Remain in Cell Cycle and Delay Differentiation

Although prior work has implicated Aurora A kinase in neuroblast cell division and self- renewal (Lee et al. 2006; Wirtz-Peitz et al. 2008; Yamada et al. 2010), the effects of Aurkb on neuroprogenitor differentiation have not been explored. Having determined that loss of FlnA or RhoA activity resulted in increased Aurkb expression during mitosis, we asked if Aurkb overexpression could reproduce the same phenotype seen with loss of function of these cytoskeletal proteins. We performed in utero electroporation of Aurkb in E13 mice and examined neural progenitor development 72 h later (Fig. 4C,D). We observed significantly more GFP$^+$ cells in the intermediate zone (IZ) of GFP-Aurkb and fewer GFP$^+$ cells in the overlying cortical plate, compared with GFP control, suggestive of reduced differentiation. Concurrently, we observed that fewer GFP$^+$ cells were present in subventricular zone of GFP-Aurkb brains (arrow heads) and more GFP$^+$ cells in Tuj1$^+$ neuronal region (arrows), compared those in control GFP brains (Fig. 4D). These findings could reflect either changes in differentiation or impaired migration. We therefore quantified the proportion of GFP-Aurkb- or control GFP-overexpressing cells that remained as progenitors (Ki67$^+$ and GFP$^+$ cells) and neuronal cells (Tuj1$^+$ and GFP$^+$) relative to the total number of transfected cells (total GFP$^+$ cells). A significantly greater proportion of transfected Aurkb cells continued to express Ki67$^+$, and a smaller proportion of Aurkb cells exited the cell cycle and entered differentiated neuronal layers (Fig. 4D graphs below), compared with control. Taken together,

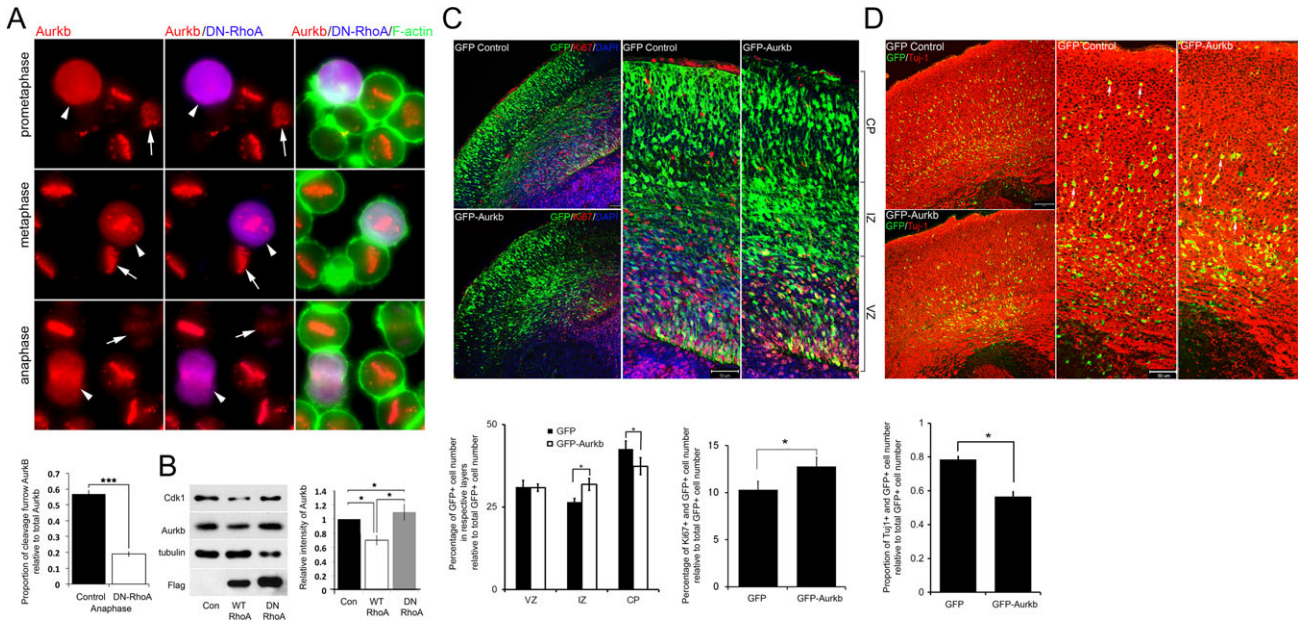

Figure 4. RhoA loss of function can disrupt Aurkb kinase localization and expression, and affect neural progenitor proliferation and differentiation. (*A*) Fluorescent photomicrographs show immunostaining for Aurkb (rhodamine) and DN-RhoA (blue) within dividing neural progenitors during various stages of the cell cycle following nocodazole release. Aurkb translocation in DN-RhoA transfected neural progenitors (arrow heads) is impaired with diffuse cytoplasmic Aurkb staining compared with that in untransfected WT cells (arrows). Changes in Aurkb localization are quantified graphically below within progenitors in anaphase. *** = $P < 0.001$. (*B*) DN-RhoA increases Auro B expression. Flag-tagged WT-RhoA or DN-RhoA was transfected into Neuro-2 cells and protein expression was checked at 12-16 h post-transfection. Western blot analyses show that DN-RhoA has higher Auro B expression, compared with that of WT-RhoA. The relative intensities of Auro B are summarized graphically on the bottom right. * = $P < 0.05$. Taken together, these observations suggest that the loss of RhoA activity impairs Aurkb translocation and degradation. (*C*) Fluorescent photomicrographs of E16 cerebral cortices 72 h after in utero electroporation of control GFP and Aurkb. Higher magnifications are shown in the right 2 panels. Fewer GFP+Aurkb expressing cells are seen in the cortical plate (and more are seen in the intermediate zone) compared with control GFP electroporations suggesting either a delay in migration or delay in differentiation. Additionally, Aurkb overexpression results in more GFP^+ and $Ki67^+$ cells relative to control GFP, suggesting that more neuroprogenitors remained in proliferative states after initial cell division. The data are represented graphically below. Collectively, these results suggest that the overexpression of Auro B kinase causes neural progenitors to remain in proliferative states, and impair their differentiation into post-mitotic neurons. * = $P < 0.05$. Scale bars = 50 μm (*D*) Co-staining of GFP (green) and Tuj1 (red) further shows that Aurkb expression affects neural progenitor differentiation at E16 cerebral cortices as described above. Fewer GFP^+ cells are seen in Tuj1-expressing cortical plate of GFP-Aurkb-electroporated brains compared with that in control GFP. Higher magnifications are shown in the right 2 panels. The proportions of GFP^+ and $Tuj1^+$ cells to total GFP^+ cells are represented graphically below. * = $P < 0.05$. Scale bars = 100 μm for left panels, and 50 μm for right panels.

these results suggest that Aurkb overexpression causes neural progenitor cells to remain as progenitors, thereby altering cell specification and their differentiation into post-mitotic neurons, much in the same manner as seen with loss of either FlnA or RhoA activity.

Discussion

Fate decision of neural progenitors during cortical development is regulated by complex intracellular factors and extracellular clues, and the molecular mechanisms underlying the fate decision remain currently major topic in neural development. Changes of spindle orientations have been suggested to dictate symmetric/asymmetric divisions and cell fate decision through segregating cell fate determinants into 2 separating daughter cells (Morin et al. 2007; Siller and Doe 2009; Streuli 2009; Morin and Bellaiche 2011). Previous studies have shown that actin-dependent cytoskeletal proteins such as FlnA can influence the transition of neural progenitors through the cell cycle by affecting the rates of degradation of cell-cycle proteins (Lian et al. 2012). Our current findings extend this role for FlnA cytoskeletal proteins by implicating a role in directing the location and expression of proteins involved in cell symmetric/asymmetric divisions and cell fate. We show that FlnA function loss increases the proportion of neural progenitors adopting symmetric divisions at mid-gestation, and so decreases the percentage of neural progenitors exiting from the cell cycle. FlnA physically and functionally interacts with RhoA. The loss of functional RhoA also prompts a reduction in neural progenitor differentiation in the same manner as FlnA loss. FlnA-dependent RhoA activity directs the translocation and degradation of cell cytokinesis associated proteins such as Aurkb during mitosis. Finally, overexpression of Aurkb leads to impairment in neural differentiation. Collectively, these studies suggest that actin-dependent proteins such as FlnA and RhoA not only regulate cell cycle progression and proliferative rates but they also mediate the expression levels and localization of cytokinesis associated determinants to influence neural cell fate.

While the current experiments demonstrate a role for FlnA in modulation of spindle orientation, FlnA may regulate cell fate decision through multiple other processes. First, FlnA regulates Cdk1 activity, which has been found to direct cell fate decision through maintaining the asymmetric localization of cell fate determinants, such as Inscuteable and Bazooka in Drosophila (Tio et al. 2001; Zhang et al. 2012, 2013). Thus, it is possible that FlnA regulates asymmetric localization of cell fate determinants via vesicle trafficking, thereby dictating cell fate decision. The effects of FlnA and RhoA on Aurkb would be consistent with this possibility. Second, it has been found that FlnA can enter the cell nucleus and bind transcription factors including the androgen receptor and Smads (Sasaki et al. 2001; Loy et al. 2003). Therefore, FlnA might regulate cell fate decision and neurogenesis at this level. Finally, integrins transmit Erk1/2 signaling into nuclei and FlnA has been found to mediate MAPK activity

(Sarkisian et al. 2006). In this regard, FlnA might regulate neurogenesis through Erk1/2 trafficking. Further studies will be needed to explore FlnA function for each of these possibilities.

Our data from pull-down and immunoprecipitation assays showed that FLNA could specifically bind to RhoA but not Rac1 and Cdc42. These results are not entirely consistent with those published previously (Ohta et al. 1999), where FLNA was found to bind to all the 3 Rho GTPases. The reason for these differences might be attributed to experimental reagents as we used FLNA C-terminal fragments but not full-length FLNA for the assays, Rac1-and Cdc42-binding sites may not be situated within the FlnA C-terminal. Nevertheless, previous works have revealed that Rho GTPases activation is dependent on filamin participation. Our work further showed that normal RhoA activity was dependent on FlnA, implying that the RhoA-FlnA association is physically and functionally essential. Another interesting observation is that the loss of RhoA activity led to a reduction in neural progenitor differentiation and fewer postmitotic neurons similar to what was seen in FlnA-null brain. Other studies have reported that Rho GTPases function as molecular switches in actin cytoskeletal remodeling and vesicle trafficking, which are crucial processes for the regulation of stem cell renewal and differentiation. Hence, our current finding, taken in the context of previous work, suggests that RhoA serves as an effector of FlnA to regulate neural progenitor fate change through affecting mitotic spindle orientation and intracellular distribution of cell fate determinants.

The mechanism by which FlnA and RhoA mediate Aurkb localization and expression is not entirely clear. The current studies do not demonstrate any direct interactions between the cytoskeletal associated proteins and the serine/threonine kinase. Although controversial, changes of spindle orientations have been suggested in several model systems (including the mammalian neuroepithelium) to dictate symmetric/asymmetric divisions and cell fate decision through segregation of cell fate determinants into 2 separating daughter cells (Morin et al. 2007; Siller and Doe 2009; Streuli 2009; Morin and Bellaiche 2011). Previous studies have shown that integrins are required for proper localization of cell fate determinants including LGN, inscuteable and par3 and spindle re-orientation (Lechler and Fuchs 2005). Moreover, in adhesion-cultured non-neural cells, integrin adhesion to extracellular matrix (ECM) orients mitotic spindles parallel to the ECM, and further the effect is dependent on participations of actin cytoskeleton and astral microtubules (Thery et al. 2005). Alternatively, the aberrant distribution and reduced degradation of Aurkb may relate to a more fundamental role for filamins in regulating actin-dependent vesicle trafficking. We have recently shown that FlnA interactions with actin-nucleating formin proteins to direct the endocytosis/exocytosis of various proteins and their transition to the lysosomal complex (Lian et al. 2016). Interestingly, RhoA GTPase activity is necessary for the release of formin autoinhibition, thereby allowing for the activation of formin domains which in turn, affect long-range actin-dependent vesicle trafficking. Hence, the loss of FlnA or RhoA activity could impair formin activation, which is necessary for intracellular trafficking and proteasomal/lysosomal degradation of various proteins, including both those implicated in cell cycle (Cdk1, catenins) and cell fate determination (Aurkb).

While formins appear to serve as downstream effectors of both filamins and Rho GTPases, how formins can regulate actin-dependent vesicle trafficking and degradation are not known. Following release of autoinhibition, it has been suggested that the proline-rich FH1 domain in Fmn2 might facilitate polymerization of actin to affect actin-dependent vesicle trafficking. The FH1 domain has been found to interact with WW domains, which are linked to E3 ubiquitin ligases and lysosomal degradation. Additional studies exploring these potential pathways may provide further insight into how cytoskeletal proteins regulate neural progenitor development.

Supplementary Material

Supplementary material is available at *Cerebral Cortex* online.

Funding

This work was supported by grants to V.L.S from NIH R01NS092062 and Grant 2016073 from the Doris Duke Charitable Foundation.

Notes

We thank Dr Takaya Satoh for the gift of RhoA, Cdc42 and Rac1 constructs and Dr Shigenobu Yonemura for anti-RhoA antibody (clone: lulu51). *Conflict of Interest*: None declared.

References

Bakal CJ, Finan D, LaRose J, Wells CD, Gish G, Kulkarni S, DeSepulveda P, Wilde A, Rottapel R. 2005. The Rho GTP exchange factor Lfc promotes spindle assembly in early mitosis. Proc Natl Acad Sci USA. 102:9529–9534.

Birkenfeld J, Nalbant P, Yoon SH, Bokoch GM. 2008. Cellular functions of GEF-H1, a microtubule-regulated Rho-GEF: is altered GEF-H1 activity a crucial determinant of disease pathogenesis? Trends Cell Biol. 18:210–219.

Bystron I, Blakemore C, Rakic P. 2008. Development of the human cerebral cortex: Boulder Committee revisited. Nat Rev Neurosci. 9:110–122.

Cappello S, Bohringer CR, Bergami M, Conzelmann KK, Ghanem A, Tomassy GS, Arlotta P, Mainardi M, Allegra M, Caleo M, et al. 2012. A radial glia-specific role of RhoA in double cortex formation. Neuron. 73:911–924.

Caviness VS Jr, Nowakowski RS, Bhide PG. 2009. Neocortical neurogenesis: morphogenetic gradients and beyond. Trends Neurosci. 32:443–450.

Chang YC, Nalbant P, Birkenfeld J, Chang ZF, Bokoch GM. 2008. GEF-H1 couples nocodazole-induced microtubule disassembly to cell contractility via RhoA. Mol Biol Cell. 19:2147–2153.

Chenn A, Walsh CA. 2003. Increased neuronal production, enlarged forebrains and cytoarchitectural distortions in beta-catenin overexpressing transgenic mice. Cereb Cortex. 13:599–606.

Chia W, Cai Y, Morin X, Tio M, Udolph G, Yu F, Yang X. 2001. The cell cycle machinery and asymmetric cell division of neural progenitors in the *Drosophila* embryonic central nervous system. Novartis Found symp. 237:139–151; discussion 151–163.

Ferland RJ, Batiz LF, Neal J, Lian G, Bundock E, Lu J, Hsiao YC, Diamond R, Mei D, Banham AH, et al. 2009. Disruption of neural progenitors along the ventricular and subventricular zones in periventricular heterotopia. Hum Mol Genet. 18:497–516.

Fox JW, Lamperti ED, Eksioglu YZ, Hong SE, Feng Y, Graham DA, Scheffer IE, Dobyns WB, Hirsch BA, Radtke RA, et al. 1998. Mutations in filamin 1 prevent migration of cerebral cortical neurons in human periventricular heterotopia. Neuron. 21:1315–1325.

Frantz GD, McConnell SK. 1996. Restriction of late cerebral cortical progenitors to an upper-layer fate. Neuron. 17:55–61.

Geschwind DH, Rakic P. 2013. Cortical evolution: judge the brain by its cover. Neuron. 80:633–647.

Gotz M, Huttner WB. 2005. The cell biology of neurogenesis. Nat Rev Mol Cell Biol. 6:777–788.

Huveneers S, Danen EH. 2009. Adhesion signaling - crosstalk between integrins, Src and Rho. J Cell Sci. 122:1059–1069.

Katayama K, Imai F, Campbell K, Lang RA, Zheng Y, Yoshida Y. 2013. RhoA and Cdc42 are required in pre-migratory progenitors of the medial ganglionic eminence ventricular zone for proper cortical interneuron migration. Development. 140:3139–3145.

Katayama K, Melendez J, Baumann JM, Leslie JR, Chauhan BK, Nemkul N, Lang RA, Kuan CY, Zheng Y, Yoshida Y. 2011. Loss of RhoA in neural progenitor cells causes the disruption of adherens junctions and hyperproliferation. Proc Natl Acad Sci USA. 108:7607–7612.

Kawajiri A, Yasui Y, Goto H, Tatsuka M, Takahashi M, Nagata K, Inagaki M. 2003. Functional significance of the specific sites phosphorylated in desmin at cleavage furrow: Aurora-B may phosphorylate and regulate type III intermediate filaments during cytokinesis coordinatedly with Rho-kinase. Mol Biol Cell. 14:1489–1500.

Kiema T, Lad Y, Jiang P, Oxley CL, Baldassarre M, Wegener KL, Campbell ID, Ylanne J, Calderwood DA. 2006. The molecular basis of filamin binding to integrins and competition with talin. Mol Cell. 21:337–347.

Kim KW, Mutter RW, Willey CD, Subhawong TK, Shinohara ET, Albert JM, Ling G, Cao C, Gi YJ, Lu B. 2007. Inhibition of survivin and aurora B kinase sensitizes mesothelioma cells by enhancing mitotic arrests. Int J Radiat Oncol, Biol, Phys. 67: 1519–1525.

Kriegstein AR, Gotz M. 2003. Radial glia diversity: a matter of cell fate. Glia. 43:37–43.

Kriegstein AR, Noctor SC. 2004. Patterns of neuronal migration in the embryonic cortex. Trends Neurosci. 27:392–399.

Lechler T, Fuchs E. 2005. Asymmetric cell divisions promote stratification and differentiation of mammalian skin. Nature. 437:275–280.

Lee CY, Andersen RO, Cabernard C, Manning L, Tran KD, Lanskey MJ, Bashirullah A, Doe CQ. 2006. Drosophila Aurora-A kinase inhibits neuroblast self-renewal by regulating aPKC/Numb cortical polarity and spindle orientation. Genes Dev. 20:3464–3474.

Lian G, Dettenhofer M, Lu J, Downing M, Chenn A, Wong T, Sheen V. 2016. Filamin A- and formin 2-dependent endocytosis regulates proliferation via the canonical Wnt pathway. Development. 143:4509–4520.

Lian G, Lu J, Hu J, Zhang J, Cross SH, Ferland RJ, Sheen VL. 2012. Filamin a regulates neural progenitor proliferation and cortical size through Wee1-dependent Cdk1 phosphorylation. J Neurosci. 32:7672–7684.

Loy CJ, Sim KS, Yong EL. 2003. Filamin-A fragment localizes to the nucleus to regulate androgen receptor and coactivator functions. Proc Natl Acad Sci USA. 100:4562–4567.

Marthiens V, ffrench-Constant C. 2009. Adherens junction domains are split by asymmetric division of embryonic neural stem cells. EMBO Rep. 10:515–520.

Morin X, Bellaiche Y. 2011. Mitotic spindle orientation in asymmetric and symmetric cell divisions during animal development. Dev Cell. 21:102–119.

Morin X, Jaouen F, Durbec P. 2007. Control of planar divisions by the G-protein regulator LGN maintains progenitors in the chick neuroepithelium. Nat Neurosci. 10:1440–1448.

Ohta Y, Suzuki N, Nakamura S, Hartwig JH, Stossel TP. 1999. The small GTPase RalA targets filamin to induce filopodia. Proc Natl Acad Sci USA. 96:2122–2128.

Palacios F, Price L, Schweitzer J, Collard JG, D'Souza-Schorey C. 2001. An essential role for ARF6-regulated membrane traffic in adherens junction turnover and epithelial cell migration. Embo J. 20:4973–4986.

Rakic P. 1988. Specification of cerebral cortical areas. Science. 241:170–176.

Roszko I, Afonso C, Henrique D, Mathis L. 2006. Key role played by RhoA in the balance between planar and apico-basal cell divisions in the chick neuroepithelium. Dev Biol. 298:212–224.

Sarkisian MR, Bartley CM, Chi H, Nakamura F, Hashimoto-Torii K, Torii M, Flavell RA, Rakic P. 2006. MEKK4 signaling regulates filamin expression and neuronal migration. Neuron. 52:789–801.

Sarkisian MR, Li W, Di Cunto F, D'Mello SR, LoTurco JJ. 2002. Citron-kinase, a protein essential to cytokinesis in neuronal progenitors, is deleted in the flathead mutant rat. J Neurosci. 22:RC217.

Sasaki A, Masuda Y, Ohta Y, Ikeda K, Watanabe K. 2001. Filamin associates with Smads and regulates transforming growth factor-beta signaling. J Biol Chem. 276:17871–17877.

Siller KH, Doe CQ. 2009. Spindle orientation during asymmetric cell division. Nat Cell Biol. 11:365–374.

Streuli CH. 2009. Integrins and cell-fate determination. J Cell Sci. 122:171–177.

Terada Y, Tatsuka M, Suzuki F, Yasuda Y, Fujita S, Otsu M. 1998. AIM-1: a mammalian midbody-associated protein required for cytokinesis. EMBO J. 17:667–676.

Thery M, Racine V, Pepin A, Piel M, Chen Y, Sibarita JB, Bornens M. 2005. The extracellular matrix guides the orientation of the cell division axis. Nat Cell Biol. 7:947–953.

Tio M, Udolph G, Yang X, Chia W. 2001. cdc2 links the Drosophila cell cycle and asymmetric division machineries. Nature. 409:1063–1067.

Toledano H, Jones DL. 2008. Mechanisms regulating stem cell polarity and the specification of asymmetric divisions. Cambridge (MA): Stem Book.

Tsuno T, Natsume A, Katsumata S, Mizuno M, Fujita M, Osawa H, Nakahara N, Wakabayashi T, Satoh Y, Inagaki M, et al. 2007. Inhibition of Aurora-B function increases formation of multinucleated cells in p53 gene deficient cells and enhances anti-tumor effect of temozolomide in human glioma cells. J Neuro-Oncol. 83:249–258.

Tungadi EA, Ito A, Kiyomitsu T, Goshima G. 2017. Human microcephaly ASPM protein is a spindle pole-focusing factor that functions redundantly with CDK5RAP2. J Cell Sci. 130:3676–3684.

Wirtz-Peitz F, Nishimura T, Knoblich JA. 2008. Linking cell cycle to asymmetric division: Aurora-A phosphorylates the Par complex to regulate Numb localization. Cell. 135:161–173.

Yamada M, Hirotsune S, Wynshaw-Boris A. 2010. The essential role of LIS1, NDEL1 and Aurora-A in polarity formation and microtubule organization during neurogensis. Cell Adh Migr. 4:180–184.

Zhang J, Neal J, Lian G, Hu J, Lu J, Sheen V. 2013. Filamin A regulates neuronal migration through brefeldin A-inhibited guanine exchange factor 2-dependent Arf1 activation. J Neurosci. 33:15735–15746.

Zhang J, Neal J, Lian G, Shi B, Ferland RJ, Sheen V. 2012. Brefeldin A-inhibited guanine exchange factor 2 regulates filamin A phosphorylation and neuronal migration. J Neurosci. 32:12619–12629.